Fast dynamics of supercoiled DNA revealed by single-molecule experiments

Aurélien Crut*, Daniel A. Koster*, Ralf Seidel*†, Chris H. Wiggins‡, and Nynke H. Dekker*§

*Kavli Institute of Nanoscience, Faculty of Applied Sciences, Delft University of Technology, Lorentzweg 1, 2628 CJ Delft, The Netherlands; and ‡Department of Applied Physics and Applied Mathematics, Columbia University, New York, NY 10027

Edited by Xiaoliang Xie, Harvard University, Cambridge, MA, and accepted by the Editorial Board May 29, 2007 (received for review January 14, 2007)

The dynamics of supercoiled DNA play an important role in various cellular processes such as transcription and replication that involve DNA supercoiling. We present experiments that enhance our understanding of these dynamics by measuring the intrinsic response of single DNA molecules to sudden changes in tension or torsion. The observed dynamics can be accurately described by quasistatic models, independent of the degree of supercoiling initially present in the molecules. In particular, the dynamics are not affected by the continuous removal of the plectonemes. These results set an upper bound on the hydrodynamic drag opposing plectoneme removal, and thus provide a quantitative baseline for the dynamics of bare DNA.

magnetic tweezers | optical tweezers | polymer dynamics

The degree of DNA supercoiling affects a number of important cellular processes, such as gene expression (1), initiation of DNA replication (2), binding kinetics of sequence-specific proteins to their targets (3), and site-specific recombination (4, 5). A strict regulation of DNA supercoiling is therefore essential for cell survival. This regulation results from a complex interplay between the occurrence of processes that generate local supercoiling of DNA, such as replication and transcription, and the action of topoisomerases, which are able to modify the global linking number (Lk) of DNA molecules via a mechanism of transient DNA strand breakage and religation (for reviews, see refs. 6 and 7).

DNA supercoiling dynamics, i.e., the rate at which supercoils are created, propagated and removed on a DNA molecule, represent an important aspect of the regulation process. This can be clearly illustrated by the example of transcription-induced supercoiling. As initially proposed by Liu and Wang (8) and confirmed by later experiments *in vitro* (9) and *in vivo* (10, 11), the inability of a transcription complex of increasing molecular weight to rotate around helical DNA results in the supercoiling of DNA in its immediate vicinity: positively supercoiled domains are generated ahead of the transcription complex, whereas negatively supercoiled domains are generated behind it. In the simple case of a single transcription complex bound to a circular DNA molecule, these supercoiled domains of opposite sign can be relaxed in one of two ways, either by the action of topoisomerases or by their mutual annihilation following their propagation along the connecting DNA segment. These two processes can have very different consequences for DNA topology: the action of topoisomerases induces a modification of Lk unless these enzymes relax positive and negative supercoils in a perfectly balanced way, whereas the merging of oppositely supercoiled domains does not influence the global Lk. Thus, the relative kinetics of these two processes appears as a major determinant of the degree of supercoiling of DNA in steady state. Within this context, DNA internal dynamics play an important role because they determine the rate at which oppositely supercoiled domains propagate and merge.

Interestingly, various *in vitro* experimental studies (9, 12, 13) have shown that the topological changes induced by transcription (in the presence of controlled topoisomerase-mediated supercoil removal rates) are significantly larger than initially predicted by Liu and Wang (8), which suggests that the propagation of supercoiled domains occurs more slowly than initially expected. Indeed, Liu and Wang described the axial rotation of DNA according to a simple model in which DNA behaves as a perfectly straight "speedometer cable" of 1 nm radius. To explain the observed experimental results, Nelson proposed that the presence of natural bends along DNA, not included in the "speedometer cable" model, may dramatically enhance the hydrodynamic drag encountered by DNA during its rotational motion (14). However, this hypothesis was challenged by recent *in vivo* studies, in which Stupina and Wang monitored the supercoiling generated on DNA rings containing a single *tetA* transcript in cells expressing gyrase but lacking DNA topoisomerase IA. In these experiments, no excess of negative supercoiling was observed, a conclusion that remained valid even in the presence of stable bends inserted into the DNA rings (15). Therefore, this particular work appears to demonstrate that, *in vivo*, the merging of oppositely supercoiled domains occurs more rapidly than the relaxation of supercoils by topoisomerases. Nonetheless, drawing quantitative conclusions about DNA internal dynamics from these experiments as well as from those cited before remains challenging, as bulk experiments, whether performed *in vivo* or *in vitro*, do not monitor dynamics directly and involve the simultaneous and interdependent action of many actors (at the very least DNA, RNA polymerases, and topoisomerases).

Here, we describe single-molecule experiments on both torsionally relaxed and torsionally constrained molecules that provide a quantitative basis for understanding DNA dynamics. The first set of experiments provides a baseline by addressing the stretching dynamics of torsionally relaxed DNA molecules following the sudden application of an external force. These experiments are facilitated by the combination of two widely used techniques, magnetic and optical tweezers. A significant advantage of this combined experimental configuration is the possibility to control the rate of DNA stretching, as the external force used to stretch DNA can be modified by more than an order of magnitude. Our results are compared with previous studies that addressed the relaxation dynamics of tethered DNA molecules (16–19). In addition, we present analytical results that, with only minimal approximations, accurately describe the quasistatic DNA dynamics observed. Using this basis, we next present results on the stretching of supercoiled DNA molecules that represent, to our knowledge, the first quantitative measure-

Author contributions: D.A.K., R.S., and N.H.D. designed research; A.C. performed research; A.C., D.A.K., and C.H.W. analyzed data; and A.C. and N.H.D. wrote the paper.

The authors declare no conflict of interest.

This article is a PNAS Direct Submission. X.X. is a guest editor invited by the Editorial Board.

Abbreviations: Lk, linking number; Wr, writhe; Tw, twist.

†Present address: Biotechnological Center, University of Technology Dresden, Tatzberg 47-51, D-01307 Dresden, Germany.

§To whom correspondence should be addressed. E-mail: n.h.dekker@tudelft.nl.

This article contains supporting information online at www.pnas.org/cgi/content/full/0700333104/DC1.

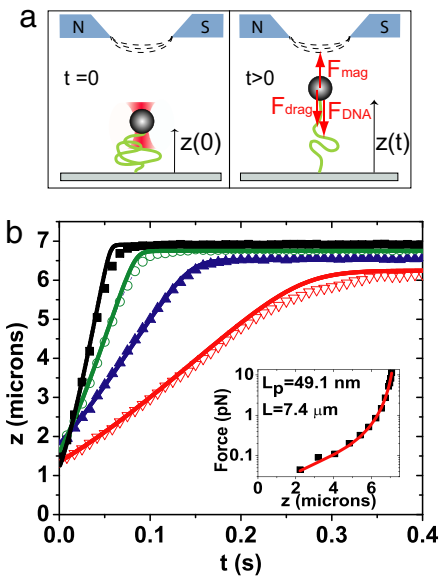

Fig. 1. Stretching experiments with torsionally relaxed DNA molecules. (*a*) Principle of the experiments: an optical trap is used to reduce the end-to-end extension of a DNA molecule attached to a magnetic bead and held under a constant external force F_{mag} (*Left*). After release of the optical trap, the end-to-end extension of the DNA molecule increases as a function of time, until it reaches its steady-state value under F_{mag}. The three forces considered in the analysis are illustrated (*Right*). (*b*) Experimental traces obtained at F_{mag} = 0.90 pN (open inverted triangles), F_{mag} = 1.48 pN (filled triangles), F_{mag} = 2.70 pN (open circles), and F_{mag} = 4.56 pN (filled squares). Data points were averaged over eight successive runs. The solid lines are obtained by solving numerically the equation of motion assuming a quasistatic behavior. (*Inset*) Black squares, experimental force-extension curve; solid red line, fit with the interpolation formula to the Worm-Like Chain model (22).

ment of the dynamics of such molecules. We investigate the sudden application of an external force to a torsionally constrained molecule, which induces a conversion of its writhe (Wr) into twist (Tw) with increasing tension (20) while maintaining a constant Lk. The analysis of these experiments shows that the frictional drag induced by this large conformational change of the DNA molecule is not large enough to alter the quasistatic character of the dynamics, and thus sets an upper bound on the drag opposing plectoneme removal. Finally, we present complementary experiments on supercoiled DNA molecules in which plectonemes are dissipated not by their conversion to Tw, but by the creation of a site-specific nick in the DNA molecule. These experiments likewise demonstrate that the process of plectoneme removal is fast compared with DNA stretching. We conclude by discussing the biological implications of the relative timescales determined.

Results

Pulling of Torsionally Relaxed DNA. Our integrated magneto-optical tweezers (described in the *Materials and Methods*) allow us to apply a nearly instantaneous force switch to a DNA molecule tethered to a magnetic bead. To do so, the extension of a DNA molecule, initially imposed by the external force created on the bead by a pair of permanent magnets, is reduced by optically trapping the bead and moving the trap position toward the surface. This leads to the initial, weakly stretched configuration illustrated in Fig. 1*a Left*. Subsequently shutting off the laser trap leads to motion of the magnetic bead back to its equilibrium position under the magnetic force F_{mag} (Fig. 1*a Right*). In this way, we can perform experiments in which DNA is stretched under the nearly instantaneous application of external forces up to 5 pN (Fig. 1*b*). As expected, at low forces (F_{mag} = 0.90 pN, red points in Fig. 1*b*), both the rate of DNA stretching and the end-to-end distance of the DNA in steady-state are lower than at high forces (F_{mag} = 4.56 pN, black points in Fig. 1*b*). Successive runs performed at a given magnetic force are highly reproducible [supporting information (SI) Fig. 7] and can therefore be averaged to reduce the effect of thermal fluctuations. The resulting traces are then analyzed using the following equation of motion obtained by balancing the forces involved (diagrammed in Fig. 1*a*)

$$F_{mag} = F_{drag}(z) + F_{DNA}(z) = \zeta_{bead}(z)\frac{dz}{dt} + F_{DNA}(z), \qquad [1]$$

where z is the distance between the surface and the nearest edge of the bead (equivalent to the DNA end-to-end distance), F_{mag} represents the external force exerted by the magnets on the bead, F_{drag} represents the hydrodynamic drag that opposes the motion of the bead, and F_{DNA} represents the force exerted by the DNA molecule on the bead. The inertia of the bead can be neglected because it contributes to a force that is several orders of magnitude smaller than the other forces involved (19). Variations of the external force experienced by the magnetic beads during their motion can also be neglected, as this external force only varies appreciably on a ≈1-mm-length scale, whereas the extent of bead motion is limited to only a few micrometers (maximally equal to the contour length L of the DNA molecules used). We note that use of Eq. **1** assumes a purely vertical motion of the bead, which is well verified experimentally, as illustrated in SI Fig. 8. The presence of the glass surface to which DNA molecules are anchored is known to lead to an enhancement of the hydrodynamic drag experienced by the bead compared with its value in bulk solution. This correction is taken into account according to the derivation by Bevan and Prieve for a motion perpendicular to the surface (21)

$$\zeta_{bead}(z) = 6\pi\eta R_b\left(1 + \frac{R_b}{z} + \frac{R_b}{2R_b + 6z}\right), \qquad [2]$$

where η is the viscosity of the buffer solution (a value of 10^{-3} kg·m^{-1}·s^{-1} was taken throughout the analysis), and R_b is the radius of the bead. With the inclusion of surface corrections, all experimental traces are described accurately using a quasistatic model. This conclusion was reached by fitting the experimentally determined force-extension curve of the molecule under study (Fig. 1*b Inset*, black points) according to the interpolation formula derived by Bouchiat *et al.* for the Worm-Like Chain elasticity (22) with DNA contour length L and persistence length l_p as parameters (Fig. 1*b Inset*, solid red line), replacing $F_{DNA}(z)$ in Eq. **1** by this optimal fit, and solving this equation numerically. The solutions to this equation (indicated by the solid traces at different magnetic forces shown in Fig. 1*b*) illustrate the excellent description of the experimental traces provided by the quasistatic model. The absence of memory effects is also supported by the fact that traces starting at different initial positions overlap well (SI Fig. 9).

Although a numerical quasistatic solution to Eq. **1** is sufficient for this analysis, we can also describe the DNA dynamics analytically using only minimal approximations. Indeed, the Worm-Like Chain elasticity of DNA can be approximated by its high-force limit $F_{DNA}(z) = k_BT/(4l_p(1 - z(t)/L)^2)$ with an error <10% for relative extensions exceeding 0.3, and in this approximation a simple analytical solution for Eq. **1** can be derived if surface effects are neglected (approximating $\zeta_{bead}(z) = 6\pi\eta R_b$):

$$\frac{tF_{mag}}{\zeta_{bead}L} = \frac{z}{L} - \frac{1}{2}\sqrt{\varepsilon}\,\tanh^{-1}\left(\frac{2(z/L) - 1}{\sqrt{\varepsilon}}\right) + C, \qquad [3]$$

where $\varepsilon = k_BT/(F_{mag}l_p)$, and C is a constant of integration. However, neglecting surface effects is unreasonable in the

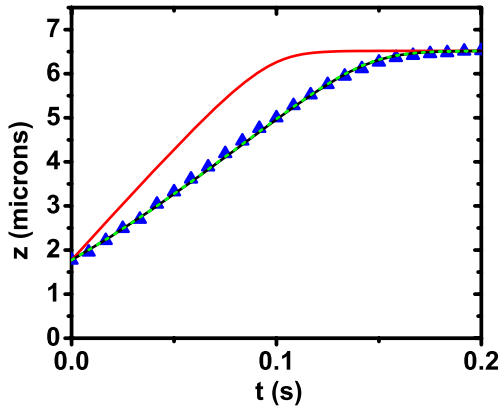

Fig. 2. Comparison of experimental data with numerical and analytical models. The experimental data presented here (blue triangles) were collected at F_{mag} = 1.48 pN. The traces issued from three models are represented: (*i*) analytical solution in the high-force approximation $F_{DNA}(z) = k_BT/(4l_p(1-z(t)/L)^2)$, without inclusion of surface effects (solid red line); (*ii*) analytical solution in the high-force approximation, with inclusion of surface effects (dashed green line); (*iii*) complete quasistatic solution of Eq. 1 obtained numerically, including the complete interpolation formula from the Worm-Like Chain model (22) and surface effects (solid black line in the background). Clearly, *i* does not provide a satisfying description of the dynamics, but *ii* and *iii* are nearly indistinguishable and in excellent agreement with the experimental data.

context of our experiments, as attested by the comparison of this analytical solution (red line in Fig. 2) with the experimental data points (blue triangles in Fig. 2). Nonetheless, as described in *SI Text*, an expanded analytical solution can also be obtained in the high-force limit when the surface effects are modeled according to Eq. **2**. Moreover, this analytical solution (dashed green line on Fig. 2) coincides almost perfectly with the numerical solution including the complete Worm-Like Chain elasticity (black line in Fig. 2).

Pulling of Supercoiled DNA. As we have shown, the stretching dynamics of torsionally relaxed DNA can be quantitatively understood by using a simple equilibrium description, providing a convenient starting point from which to test the more complicated behavior of supercoiled DNA. These experiments are conducted in a manner similar to those involving torsionally relaxed DNA, except that the Lk of the molecule under study is modified by a rotation of the magnets before stretching. The starting configuration of these experiments is thus a weakly stretched DNA molecule containing plectonemic structures, as illustrated in Fig. 3*a Left*. Because the magnets are held fixed after the initial application of supercoils into the DNA, the Lk of the DNA molecules is fixed during the stretching phase (Fig. 4, "force switch" arrow). However, because the partition between Tw and Wr depends on the tension along the DNA molecule (20, 23), the final steady-state conformation of the DNA molecule is expected to include a reduced number of plectonemes compared with its initial configuration. The dynamics of this Wr to Tw conversion necessarily involves the rotation of the plectonemes about their axis (Fig. 3*a Right*). The experimental traces as a function of increasing magnetic force are shown in Fig. 3*b* (F_{mag} = 2.20 pN, red points; F_{mag} = 2.72 pN, blue points; F_{mag} = 3.36 pN, green points; F_{mag} = 4.14 pN, black points). As in the case of relaxed DNA, the DNA stretching rate is observed to increase with increasing applied magnetic force.

We find that the dynamics of covalently closed, supercoiled DNA under an applied magnetic force are also well described by a quasistatic model. Numerical modeling in the absence of DNA internal dynamics proceeded as in the case of relaxed DNA, with one exception. Although, in the case of relaxed DNA, an

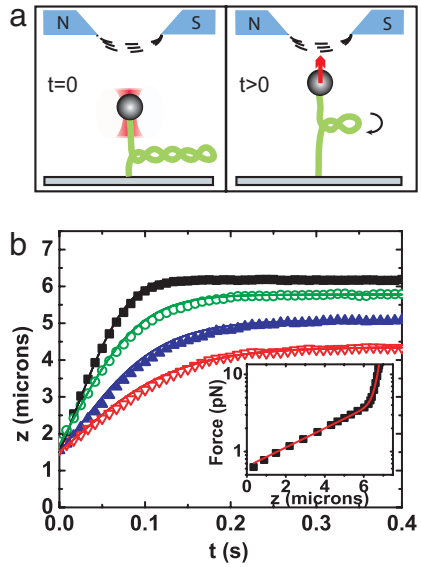

Fig. 3. Stretching experiments with supercoiled DNA molecules. (*a*) These experiments are similar to those involving torsionally relaxed DNA (Fig. 1), except that plectonemes have been created in the initial configuration by a preliminary rotation of the magnets (*Left*). The stretching phase involves the conversion of plectonemic structures into twist (*Right*). (*b*) Experimental traces (data points averaged over eight successive runs) obtained at F_{mag} = 2.20 pN (open inverted triangles), F_{mag} = 2.72 pN (filled triangles), F_{mag} = 3.36 pN (open circles), and F_{mag} = 4.14 pN (filled circles). The linking number of the molecule had been modified by + 100 turns before these pulling experiments. The solid lines are obtained by solving numerically the equation of motion assuming a quasistatic behavior. (*Inset*) Black squares, experimental equilibrium force-extension curve with ΔLk = +100; solid red line, biexponential fit. More details about the static behavior of supercoiled DNA in various conditions can be found in ref. 20.

interpolation formula for the molecule's elasticity exists, there is no complete description of a molecule's elasticity as a function of force at nonzero torque. Therefore, we opted to describe the

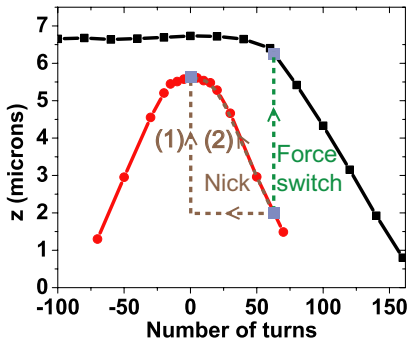

Fig. 4. Scenarios of experiments involving supercoiled DNA. The experimentally measured DNA extension at equilibrium for different values of its linking number (0 turn represents a torsionally relaxed molecule) is illustrated for F_{mag} = 1.7 pN (filled squares), and F_{mag} = 0.35 pN (filled circles). The blue squares indicate initial and final configurations in the two types of experimental situations described in this paper. Force switch experiments take place at constant linking number but involve an increase of the tension along DNA (green dashed line). On the contrary, in relaxation experiments the initial and final tensions are equal, but the initial torsional constraint is totally relaxed in the final state. This transition can *a priori* occur in two different ways (brown dashed lines): in the first scenario (1), plectoneme relaxation is much faster than DNA stretching, so that most of the motion involves torsionally relaxed DNA. In the second scenario (2), DNA stretching is faster than plectoneme relaxation so that plectonemes are progressively removed during the experiment.

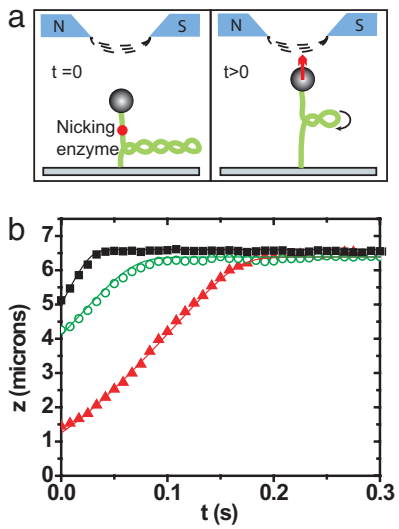

Fig. 5. Relaxation of supercoils by a nicking enzyme. (*a*) Principle of the experiments: the linking number of a DNA molecule is initially modified to create plectonemes. Experiments take place in the presence of nicking enzymes N.BbvCIA (*Left*). DNA extension shows a sudden increase after a nick is induced by one of these enzymes (*Right*). (*b*) Individual experimental traces obtained with $F_{mag} = 2.5$ pN and $\Delta Lk = +100$ turns (filled squares), $F_{mag} = 1.4$ pN and $\Delta Lk = +100$ turns (open circles) and $F_{mag} = 1.4$ pN and $\Delta Lk = +200$ turns (filled triangles). Time $t = 0$ corresponds to the action of the nicking enzyme. The solid lines are obtained by solving the equation of motion for torsionally relaxed DNA molecule, assuming quasistatic dynamics.

experimentally determined equilibrium force-extension behavior (Fig. 3*b Inset*, black points) phenomenologically, by fitting it to a double exponential relation (Fig. 3 *b Inset*, solid red curve). The resulting best fit to the data was then substituted into $F_{DNA}(z)$ in Eq. **1**. The solid curves shown in Fig. 3*b* represent the dynamical behavior predicted according to this model, which, as in the case of torsionally relaxed DNA, indicates that the experimental data are well described by a quasistatic model.

Relaxation of Supercoiled DNA. In addition to probing the dynamics of plectonemic supercoil removal by stretching, we also study its dynamics after the abrupt release of the torsional constraint. In this case, supercoiled DNA molecules are initially tethered as before and held under a constant magnetic force (Fig. 5*a Left*). In the presence of the nicking enzyme N.BbvCIA, whose target site occurs only once in the 20-kb DNA molecules used in our experiments, cleavage of a single DNA strand by the nicking enzyme removes the torsional constraint imposed by the magnets. This allows the molecule to release its torsional stress by a relative rotation of the two DNA strands, changing Lk in the process and resulting in a reduction in the number of plectonemic supercoils (Fig. 5*a Right*). The resulting upward motion (Fig. 5*b*) shows how the resulting dynamics vary as a function of force (compare traces with ΔLk = 100 turns at $F_{mag} = 1.4$ pN, green points, and with ΔLk = 100 turns at $F_{mag} = 2.5$ pN, black points) and as a function of initial number of supercoils (compare traces with $F_{mag} = 1.4$ pN and ΔLk = 100 turns, green points and with $F_{mag} = 1.4$ pN and ΔLk = 200 turns, red points). Interestingly, for all of the conditions tested (including a reduction of the bead size by a factor of 3, data not shown), a successful description of the DNA extension trajectories in time is obtained by only taking into account the quasistatic stretching of torsionally relaxed DNA (Fig. 5, solid lines). As described in *Discussion*, these results indicate that plectoneme removal must occur on a time scale that is significantly faster than the upward movement of the bead due to the stretching, placing a lower bound on its rate.

Discussion

A large part of the results described here was obtained by the use of an apparatus that combines optical and magnetic tweezers. Although the building of a similar experimental configuration has been reported in previous studies (24, 25), our work constitutes its application to the study of a biologically relevant problem. This setup unites two features that are essential for studying the intrinsic dynamics of supercoiled DNA: first, the ability to twist DNA, provided by the magnetic tweezers, and second, the possibility to apply a sudden force switch. Whereas classical magnetic tweezers do not meet this second requirement, because changes in the magnetic force are typically obtained only through the slow translation of the permanent magnets, laser traps can be switched on and off within a few milliseconds using a commercial shutter. An additional advantage of these experiments is that two parameters are directly available to control the dynamics, the initial extension of DNA and the force used for DNA stretching. In comparison, relaxation experiments have only one readily accessible parameter that influences the dynamics, namely the initial extension of DNA.

The dynamics of torsionally relaxed DNA have been previously studied in two ways. In a first approach, the relaxation of hydrodynamically stretched, fluorescently labeled DNA molecules was monitored by fluorescence microscopy (26). In a second approach, a DNA molecule attached to a bead was initially stretched by optically trapping the bead, and relaxed to an unstretched configuration following trap release (16–19). The physics probed in the two situations is very different: whereas, in the first case, the relaxation dynamics of a DNA molecule is strongly out of equilibrium and governed by tension propagation along the molecule (27, 28), in the second configuration the presence of a bead and its associated hydrodynamic friction considerably slows down the motion, and quasistatic dynamics are thus expected to describe the motion of the DNA-bead complex (19). Nonetheless, whether this is actually the case has been a long-standing debate. Early results were only adequately described by the quasistatic model upon assuming a 3-fold higher value of the DNA persistence length than that commonly accepted (16). Later, Bohbot-Raviv *et al.* (17) developed a model including nonequilibrium effects to explain an apparent discrepancy of their data with the quasistatic model. However, it was subsequently established that the apparent discrepancy was not attributable to nonequilibrium effects, but rather to the effect of the surface on the effective hydrodynamic drag of the bead (18, 19). In the present work, we observed an excellent agreement between the experimental traces and the predictions of the quasistatic model. This agreement was observed over a large range of stretching velocities (up to $\approx$100 μm/s), due to our ability to tune the magnetic force that drives DNA stretching (cf. Eq. **1** and traces from Fig. 1), whereas classical relaxation experiments, in which dynamics reduces to $\zeta_{bead}(z)\ dz/dt = F_{DNA}(z)$, lack an equivalent parameter to easily influence the motion velocity.

The dynamical behavior of supercoiled DNA differs fundamentally from that of torsionally relaxed DNA, as the elongation of a supercoiled DNA molecule requires the removal of its plectonemic structures, both when the motion is driven by a force switch (Fig. 3) and by the action of a nicking enzyme (Fig. 5). Thus, it was not *a priori* clear which of the two processes, DNA stretching (governed, as demonstrated in the previous section by the magnetic force, by the hydrodynamic drag on the bead and the DNA elasticity) and plectoneme removal, would dominate the elongation kinetics. Our experiments provide an unambiguous answer to this question: under the experimental conditions tested, we never observed any influence of plectoneme removal on the elongation kinetics.

In experiments in which a sudden increase of the force exerted on a supercoiled DNA molecule is imposed, plectoneme removal is induced by DNA stretching. This causes a progressive increase of the tension along DNA and mediates the conversion of its Wr into Tw. The good fit of the experimental data to a quasistatic model implies that the internal dynamics of DNA, which includes plectoneme removal, is so rapid that the DNA molecule is effectively always in an equilibrium configuration. The nature of the motion induced by the action of a nicking enzyme on supercoiled DNA is different, as in this configuration plectoneme removal can in principle occur independently of DNA stretching. Two principal scenarios are *a priori* plausible in these experiments (Fig. 4). The first one (Fig. 4, path 1) assumes that plectoneme removal is much faster than DNA stretching; in this case the greater part of the observed motion takes place at $\Delta Lk \approx 0$. In the second scenario (Fig. 4, path 2), plectoneme removal is rate-limiting; in this case, the tension along DNA remains always close to F_{mag}, so that the rate of the DNA extension is expected to be slow (cf. Eq. **1**). Because our experiments are accurately described with the model used to describe the dynamics of torsionally relaxed DNA (Fig. 5), the first scenario, in which the rate of plectoneme removal exceeds the rate of DNA stretching, applies. Therefore, the dynamics are governed by the rate of DNA stretching rather than the rate of plectoneme removal in both the force switch and nicking enzyme experiments, even though the manner in which plectonemes are removed differs in the two cases.

To quantitatively understand the observed separation of time scales between plectoneme removal and DNA stretching in both experiments on supercoiled DNA, it is useful to estimate the drag torque that a plectonemic region can exert during its shortening. As the starting point of this analysis, we calculate this torque in a simple model under the assumptions that the supercoiled DNA molecule contains a single branch of plectonemes (simulations clearly exclude the other extreme, in which the DNA contains as many branches as individual plectonemes) and that the shortening of this region involves its global rotation. The rotation around a given axis of a rigid but not necessarily straight DNA fragment of diameter d and length L_{plect} at an angular velocity ω encounters a hydrodynamic drag μ_{drag}, which depends crucially on the fragment distribution relative to the rotation axis and contributes to the following torque (14):

$$\tau_{drag} = \mu_{drag}\omega L_{plect}\langle r_{\perp}^2\rangle, \qquad [4]$$

where $\mu_{drag} = 4\pi\eta/(0.8+\ln(X/d))$ (29). In this equation, $r_{\perp}$ is the distance of a DNA point to the rotation axis, brackets represent the average along the whole DNA fragment, and X is a cutoff length representing the distance over which a DNA fragment is straight. Nelson (14) proposed to equate X with the structural persistence length of DNA, equal to 130 nm. Nonetheless the weak dependence of μ_{drag} on X implies that its precise numerical value does not play an important role. Using the simple model detailed in ref. 30 to describe a DNA molecule under tension F and torsion, one can obtain an analytical expression for the plectonemic radius $R_{plect} = (k_BTl_p/2F)^{1/2}$. One can then replace $\langle r_{\perp}^2\rangle$ in the expression of τ_{drag} by $R_{plect}^2/2$.

Force switch experiments are then reanalyzed by including the additional force term τ_{Drag}/R_{plect} contributed by the rotating plectonemes in Eq. **1**. As before, the resulting equation of motion is solved numerically, again assuming that the configuration of DNA at a given extension is the same as at equilibrium. This analysis indicates that the rotational drag opposing plectoneme rotation is not expected to significantly affect the dynamics within the context of the model described above, because the predicted extension versus time (Fig. 6, red trace) almost precisely overlaps with predictions in which this drag torque is ignored (Fig. 6, black trace). Nonetheless, it can be concluded

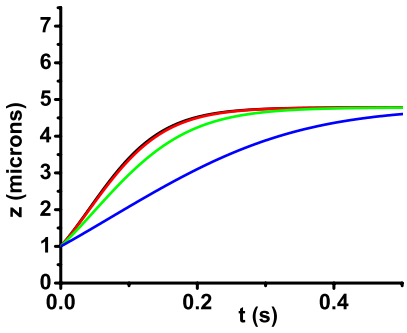

Fig. 6. Predicted stretching behavior of supercoiled DNA following a sudden force switch, as a function of the magnitude of the hydrodynamic drag induced by plectonemes. In this example, $F_{mag} = 2.5$ pN and $\Delta Lk = +100$ turns. The hydrodynamic drag opposing plectoneme removal corresponding to the simple model described in the text has been added in the equation of motion (1). Numerically solving this equation (red line) shows that this leads only to a nearly indistinguishable modification of the quasistatic dynamics (black line). However, traces generated by arbitrarily considering 10-fold (green line) and 50-fold (blue line) larger hydrodynamic drags are significantly different.

that the rotational drag opposing plectoneme rotation would have a discernable effect if it were 10 times or more larger (Fig. 6, green trace, 10-fold larger drag; blue trace, 50-fold larger drag; these traces do not refer to a specific model for plectoneme relaxation, but are drawn as references to estimate the minimal detectable drag in our experiments). Thus, these experiments allow us to place an upper bound on the rotational drag presented by plectonemic supercoils.

The relaxation experiments are analyzed using the same framework in a more straightforward manner. A direct estimation of the time scale of plectoneme removal is obtained by equating the torque driving plectoneme relaxation, equal to $(2k_BTl_pF_{mag})^{1/2}$ in the initial configuration (30) with the drag torque τ_{drag} opposing it. One gets $\omega = 4\ 2^{1/2}\ (k_BTl_p)^{-1/2}F_{mag}^{3/2}/(\mu_{drag}L_{plect})$. Using typical experimental parameters ($F_{mag} = 1.5$ pN, $L_{plect} = 5$ μm at $t = 0$) yields an initial value of the initial angular velocity $\omega \approx 610^4$ rad/s. This rate is expected to be enhanced as the size of the plectonemic region decreases. In this model, the total removal of 200 plectonemic units is accomplished within $T \approx 10$ ms, similar to the acquisition time in our experiments and much shorter than the total duration of DNA stretching under these conditions (typically 0.1 s, cf. Fig. 5). Similarly to force switch experiments, our data are therefore consistent with the simple model described by Eq. **4**, but disagree with a rotational drag larger by 10 times or more than the prediction of this simple model. These experiments therefore exclude models for plectoneme relaxation that would generate a global friction larger by a factor of 10 or more than the simple model above, caused for instance by large intrinsic bends in the plectonemic region.

Thomen *et al.* (31) have addressed the rotational drag of a double-stranded DNA molecule during its unzipping, and showed that the induced drag of such a relatively simple structure deviated from the naïve "speedometer model" of Levinthal and Crane (32) by only a factor of 10. Our experiments complement this work by addressing the rotational drag of plectonemic structures in a number of different cases, and place an upper bound on its value. Together, these experiments provide the main features of the dynamics of an individual DNA molecule under torsion and exclude a large contribution of DNA intrinsic bends to these dynamics. An interesting perspective of our work is offered by its potential extension to situations in which DNA interacts with proteins. For instance, stretching and nicking experiments may be performed in the presence of transcription complexes, nucleosomes or more generally DNA-binding pro-

teins. This might considerably slow down the dynamics, as suggested by Leng and McMacken from bulk *in vitro* experiments (33). It is likely that these experiments will have to be analyzed using the theoretical framework of Nelson's work (14), contrary to the ones presented here. Such experiments have the potential to provide a quantitative description of many aspects of supercoiled DNA dynamics that are difficult to extract from bulk experiments.

Materials and Methods

Experimental Setup. All experiments were performed with 20.7 kb long DNA molecules containing a unique site for the nicking enzyme N.BbvCIA. The two ends of the molecules were ligated to 0.6-kb-long biotin and digoxigenin PCR fragments, respectively. The DNA molecules were incubated with streptavidin-functionalized Micromer magnetic beads (3 μm diameter, Micromod, Rostock, Germany) selected for their low magnetic content, which permitted good optical trapping, and introduced in a custom-made flow cell. The lower slide of the flow cell was coated with polystyrene (1% wt/vol in toluene), anti-digoxygenin (50 μg/ml in PBS), and finally polyglutamic acid (50 mg/ml in PBS); the latter step aimed at reducing nonspecific interactions.

The detailed experimental configuration of the magnetic tweezers has been described (23). Briefly, a pair of magnets was used to apply forces and rotations to a magnetic bead bound to a tethered DNA molecule to control the tension and the linking number the DNA molecules. The bead's 3D position was determined with 10 nm accuracy from the video images with an acquisition frequency of 120 Hz. The force corresponding to a given position of the magnets was measured from the lateral fluctuations of the bead. The standard magnetic tweezers setup was expanded to include an optical trap. An infrared laser beam (1,064 nm, 500 mW; Crystalaser, Reno, NV) was attenuated to 50–100 mW and expanded through a 10× beam expander (CVI, Albuquerque, NM) to fill the back aperture of the objective (N.A. 1.4, 100×; Olympus, Netherlands). This generated a strongly focused spot in the flow cell, which was vertically translated using the piezoelectric objective positioner (Physik Instrumente, Karlsruhe, Germany) and switched on and off using a shutter (Melles Griot, Rochester, NY) inserted along the optical path.

Force Switch Experiments. These experiments were carried out in 10 mM Phosphate Buffer pH 7.4, 10 mM Sodium Azide, 0.1% Tween 20 and 200 μg/ml BSA. The magnets were first translated and rotated until the desired values for the magnetic force and the DNA linking number were reached. Then the bead under study was optically trapped and brought closer to the surface by vertical translation of the optical trap. The trap was suddenly switched off by triggering the closure of the shutter located in the optical path. Afterward, the bead moved up until it reached again its equilibrium position under the magnetic force (Figs. 1 and 3). In these experiments, the position of the optical trap was carefully adjusted to minimize the lateral motion of the bead, as the analysis was facilitated by the assumption that the bead primarily executed vertical motion away from the surface (SI Fig. 9). Eight successive traces were taken and averaged for each experimental condition tested.

Experiments with the Nicking Enzyme N.BbvCIA. These experiments were performed in a buffer containing 10 mM Tris-HCl pH 8.0, 50 mM NaCl, 10 mM $MgCl_2$, 1 mM DTT, 0.1% Tween 20, 200 μg/ml BSA, 10% 10X T4 DNA Ligase Buffer (New England Biolabs, Ipswich, MA), 0.5 units/μl of the nicking enzyme N.BbvCIA and 4 10^{-4} units/μl of T4 DNA Ligase (both enzymes from New England Biolabs). The simultaneous presence of nicking enzyme and ligase allowed us to acquire multiple traces with the same molecule, using the following procedure: first, the magnets were rotated to induce supercoils in the DNA. Second, after a time interval, single-strand cleavage by the nicking enzyme caused the DNA to relax to a torsionally unconstrained state. After a subsequent time interval necessary for ligase to repair the created nick, magnet rotation was used to induce supercoils again. Successive experiments were very reproducible in these conditions.

We thank Ya-Hui Chien and Susanne Hage for preparing the DNA constructs, Alexander Vologodskii for numerical simulations of the number of plectoneme branches, Cyril Claudet for helpful technical advice, and Derajavan Thirumalai, Alexander Vologodskii, and David Bensimon for useful discussions. N.H.D. acknowledges financial support from the Foundation for Fundamental Research on Matter and the Netherlands Organization for Scientific Research.

1. Fisher LM (1984) *Nature* 307:686–687.
2. Funnell BE, Baker TA, Kornberg A (1987) *J Biol Chem* 262:10327–10334.
3. Gowers DM, Halford SE (2003) *EMBO J* 22:1410–1418.
4. Vologodskii A, Cozzarelli NR (1996) *Biophys J* 70:2548–2556.
5. Huang J, Schlick T, Vologodskii A (2001) *Proc Natl Acad Sci USA* 98:968–973.
6. Wang JC (1996) *Annu Rev Biochem* 65:635–692.
7. Champoux JJ (2001) *Annu Rev Biochem* 70:369–413.
8. Liu LF, Wang JC (1987) *Proc Natl Acad Sci USA* 84:7024–7027.
9. Tsao YP, Wu HY, Liu LF (1989) *Cell* 56:111–118.
10. Wu HY, Shyy SH, Wang JC, Liu LF (1988) *Cell* 53:433–440.
11. Giaever GN, Wang JC (1988) *Cell* 55:849–856.
12. Droge P, Nordheim A (1991) *Nucleic Acids Res* 19:2941–2946.
13. Wang Z, Droge P (1997) *J Mol Biol* 271:499–510.
14. Nelson P (1999) *Proc Natl Acad Sci USA* 96:14342–14347.
15. Stupina VA, Wang JC (2004) *Proc Natl Acad Sci USA* 101:8608–8613.
16. Feingold M (2001) *Physica E* 9:616–620.
17. Bohbot-Raviv Y, Zhao WZ, Feingold M, Wiggins CH, Granek R (2004) *Phys Rev Lett* 92:098101.
18. Coelho Neto J, Dickman R, Mesquita O (2005) *Physica A* 345:173–184.
19. Goshen E, Zhao WZ, Carmon G, Rosen S, Granek R, Feingold M (2005) *Phys Rev E Stat Nonlin Soft Matter Phys* 71:061920.
20. Strick TR, Allemand JF, Bensimon D, Croquette V (1998) *Biophys J* 74:2016–2028.
21. Bevan M, Prieve D (2000) *J Chem Phys* 113:1228–1236.
22. Bouchiat C, Wang MD, Allemand J, Strick T, Block SM, Croquette V (1999) *Biophys J* 76:409–413.
23. Strick TR, Allemand JF, Bensimon D, Bensimon A, Croquette V (1996) *Science* 271:1835–1837.
24. Sacconi L, Romano G, Ballerini R, Capitanio M, De Pas M, Giuntini M, Dunlap D, Finzi L, Pavone F (2001) *Opt Lett* 26:1359–1361.
25. Claudet C, Bednar J (2005) *Appl Opt* 44:3454–3457.
26. Perkins TT, Quake SR, Smith DE, Chu S (1994) *Science* 264:822–826.
27. Brochard-Wyart F (1995) *Europhys Lett* 30:387–392.
28. Manneville S, Cluzel P, Viovy J, Chatenay D, Caron F (1996) *Europhys Lett* 36:413–418.
29. Hunt AJ, Gittes F, Howard J (1994) *Biophys J* 67:766–781.
30. Charvin G, Allemand J, Strick T, Bensimon D, Croquette V (2004) *Contemp Phys* 45:383–403.
31. Thomen P, Bockelmann U, Heslot F (2002) *Phys Rev Lett* 88:248102.
32. Levinthal C, Crane HR (1956) *Proc Natl Acad Sci USA* 42:436–438.
33. Leng F, McMacken R (2002) *Proc Natl Acad Sci USA* 99:9139–9144.